Combined estimation of effective electrical conductivity and permittivity for soil monitoring

A. Brovelli[a,b#] and G. Cassiani[b]

[a] Laboratoire de technologie écologique, Institut d'ingénierie de l'environnement, Station No. 2, Ecole Polytechnique Fédérale de Lausanne, CH-1015 Lausanne, Switzerland. (alessandro.brovelli@epfl.ch).

[b] Dipartimento di Geoscienze, Università di Padova, Via Gradenigo 6, 35121 Padova, Italy (giorgio.cassiani@unipd.it).

Accepted for publication on *Water Resources Research*

13 June 2011

Corresponding author. Phone +41-(0)21-6935919, Fax +41-(0)21-6938035

ABSTRACT

The mapping of moisture content, composition and texture of soils is attracting a growing interest, in particular with the goal of evaluating threats to soil quality, such as soil salinization. Fast non-invasive geophysical surveys are often used in this context. The aim of this work was to study constitutive models that can be used to parameterize electrical conductivity and permittivity starting from a unifying conceptual approach, and to evaluate whether the information carried by one measurement type can be used to identify soil parameters that are then used to predict the other geophysical quantity. To this end, a recently-developed constitutive model was here extended and modified to consider also the grain surface conductivity, a critical component in most natural situations. The extended model was successfully tested against laboratory measurements. In addition, the new model was compared against five other equations that use similar soil parameterizations. It was concluded that only three out of the five selected models yield similar predictions, while the remaining two predict a different geophysical response for the same soil texture. Following this analysis, a methodology was developed to estimate soil salinity starting from the simultaneous measurements of bulk electrical conductivity and permittivity and validate this methodology against laboratory experiments. The method is valid in situations where the conductivity of the pore-water remains approximately constant during the measurement period. Key features of the approach proposed to map soil salinization are (i) simplicity, (ii) absence of fitting parameters and (iii) the fact that moisture content does not need to be measured or estimated independently. The methodology was tested on a large number of soil samples and proved robust and accurate.

Keywords: hydrogeophysics, moisture content, non-invasive measurements, TDR, Archie's law, Topp equation, dielectric constant, surface conductivity, salinization, digital soil mapping.

1. Introduction

Characterization of soil texture and monitoring of soil state are extremely important in the perspective of sustainable development, for example to preserve fertility of agricultural areas and to identify possible threats for the near surface environment, including a number of hydrological impacts. In this context, geophysical methods are used to estimate and map key soil properties, including clay and organic matter content, moisture dynamics, rooting depth, salinity and redox state [e.g. *Abdel Aal et al.*, 2004; *Atekwana*, 2010; *Benderitter and Schott*, 1999; *Binley et al.*, 2002; *Cassiani et al.*, 2006, 2009; *Corwin et al.*, 2003; *Corwin and Lesch*, 2005a,b; *Dannowski and Yaramanci*, 1999; *Day-Lewis and Singha*, 2008; *Friedman*, 2005; *Hayley et al.*, 2009; *Hubbard et al.*, 2001; *Kästner and Cassiani*, 2009; *Koestel et al.*, 2008; *Koestel et al.*, 2009a,b; *Müller et al.*, 2010; *Schwartz et al.*, 2008; *Shevnin et al.*, 2007]. Amongst the most used geophysical tools are electrical resistivity tomography (ERT), ground penetrating radar (GPR) and time-domain reflectometry (TDR) [*Rubin and Hubbard*, 2005; *Vereecken et al.*, 2006]. These geophysical techniques measure the electromagnetic properties of the soil – DC electrical conductivity for ERT, and permittivity for GPR [e.g. *Huisman et al.*, 2003] and TDR [e.g. *Robinson et al.*, 2003]– and rely on constitutive equations to recover variables of environmental significance from the measurements [*Day-Lewis et al.*, 2005; *Rubin and Hubbard*, 2005]. Classical models used to link DC electrical conductivity to moisture content such as *Archie's* law [1942] and its extensions are often modified to account for the effect of surface and grain conductivity [*Clavier et al.*, 1984; *De Lima and Sharma*, 1990; *Glover et al.*, 2000; *Pride*, 1994; *Waxman and Smits*, 1968]. The *Topp et al.*, [1980] equation and the complex refractive index model (CRIM) [*Birchack et al.*, 1974, *Brovelli and Cassiani*, 2008; *Roth et al.*, 1990] are the relationships most frequently used to analyze the permittivity of variably-saturated porous

materials. Innovative methodologies – in particular joint inversion schemes – have been recently proposed with the aim to integrate information and measurements obtained from surveys conducted using different tools, such as measurements of electrical conductivity, permittivity, EM wave velocity and *in situ* soil state variables (salinity, moisture content, etc.) [e.g. *Binley et al.*, 2001; *Gallardo and Meju*, 2004; *Hinnell et al.*, 2010; *Linde et al.*, 2006; *Looms et al.*, 2008; *Rings et al.*, 2010; *Vereecken et al.*, 2006]. These approaches are receiving increasing attention because, being based on more abundant and diversified pieces of information, they potentially provide a more accurate and reliable imaging of the characteristics of the subsurface. Nearly all the data integration schemes rely on petrophysical constitutive models to link the different datasets: the constitutive model is either chosen *a priori* [e.g. *Binley et al.*, 2001; *Hinnell et al.*, 2010; *Looms et al.*, 2008; *Rings et al.*, 2010; *Rubin and Hubbard*, 2005; *Vozoff and Jupp*, 1975] or a 'structural' approach is used, that is, a common geometry is assumed and the link between the measured physical properties is derived based on the results of the joint inversion [*Gallardo and Meju*, 2004; *Haber and Oldenburg*, 1997; *Linde et al.*, 2006]. In this second case, the petrophysical equations are used to gain insights into the physical, chemical and hydrological properties of the subsurface. The availability of reliable, physically based constitutive models is therefore of paramount importance for the success of any data integration schemes.

DC electrical conductivity and high-frequency permittivity as obtained respectively from ERT and TDR/GPR surveys, are two inter-related variables – that is, they depend, to some extent, on the same soil characteristics – and have been often combined to map texture and moisture content [*Binley et al.*, 2001; *Linde et al.*, 2006; *Looms et al.*, 2008]. Owing to this similarity, the relationship between effective conductivity and permittivity has been proposed as a viable tool to map soil salinity, and few empirical equations have been proposed to construct a

89 'soil salinity index' [*Hamed et al.*, 2003; *Hilhorst*, 2000; *Malicki and Walczak*, 1999]. Some
90 petrophysical laws exist to model these two quantities with the same parameterization, linking
91 the soil bulk response to its moisture content and to the geometry of the pore-space (porosity and
92 connectivity). From a pore-scale perspective, bulk soil electrical conductivity and permittivity
93 are different in that the electrical conductivities of the solid (skeleton) and gaseous phases are
94 negligible, whereas permittivity is not. On the contrary, electrical conductivity is often
95 influenced by the conductance arising from the excess of charge in the vicinity of the negatively
96 charged solid surfaces of silica, clays and organic matter [*Brovelli et al.*, 2005; *Revil and Glover*,
97 1997; *Revil et al.*, 1998]. The additional contribution of the charged interface is often converted
98 into an equivalent grain (volumetric) conductivity [*Bussian*, 1983; *De Lima and Sharma*, 1990],
99 and therefore analogous boundary value problems can describe both bulk permittivity and
100 electrical conductivity [*Brovelli and Cassiani*, 2010b; *Brovelli et al.*, 2005; *Linde et al.*, 2006].
101 Although developed using different approaches, including empirical or semi-empirical
102 considerations [*Archie*, 1942; *Clavier et al.*, 1984; *Waxman and Smits*, 1968], effective medium
103 theories [*Bussian*, 1983; *Miller*, 1969; *Sen et al.*, 1981] and volume-averaging algorithms [*Linde*
104 *et al.*, 2006; *Pride*, 1994], most of the petrophysical equations suited to model both DC electrical
105 conductivity and high-frequency permittivity utilize a parameterization that is compatible with
106 that introduced by *Archie* [1942]. In other words, all these models use a parameter to describe
107 the inner topology of the pore-space (tortuosity and connectivity) that can be correlated to
108 Archie's cementation factor m, while the effect of water saturation is described by a saturation
109 exponent n that depends on the pore-size distribution and the properties
110 (wettability/hydrophobicity) of the inner surface of the porous medium [*Chen and Or*, 2006;
111 *Knight and Abad*, 1995; *Robinson and Friedman*, 2001; *Suman and Knight*, 1997].

Recently, *Brovelli and Cassiani* [2010b] proposed a novel mixing equation to compute the permittivity of geological mixtures using the same parameters introduced by *Archie* [1942]. The model was applied to study the electromagnetic properties of clean porous materials, that is, materials with negligible clay content and, therefore, negligible grain surface conductance. Comparison with experimental data in both saturated and variably saturated conditions demonstrated the excellent predicting capabilities of the model, even when *all model parameters* were independently measured.

The objectives of this work were:

1. to extend the model of *Brovelli and Cassiani* [2010b] to consider also the grain surface conductivity;
2. to verify whether the extended model can predict electrical conductivity and permittivity of soils and other geological materials where the contribution of the matrix to the bulk electrical conductivity cannot be neglected;
3. to analyze some of the other existing petrophysical laws based on the same parameterization, in order to ascertain whether the relevant calibrated parameters can be reliably used to estimate the physical properties of the soil;
4. to identify the petrophysical models that are best suited to data fusion and joint inversion schemes, including our proposed extended model;
5. to derive a relationship between bulk electrical soil properties – DC electrical conductivity and permittivity in the static limit – that can be used to map soil salinity and pore-water conductivity with fast, non invasive soil mapping surveys.

2. Petrophysical model

2.1 Model overview

The petrophysical constitutive model of *Brovelli and Cassiani* [2010b] was developed by combining variational bounds for the transport properties of granular composites [*Hashin and Shtrikman*, 1962; *Milton*, 1981] and *Archie*'s [1942] law, a constitutive model commonly used to parameterize electrical conductivity of variably saturated porous media. The model was consistently developed for two- and three-phase materials on the basis of the same basic assumptions. In the following, only the key model equations are presented, as full details can be found in *Brovelli and Cassiani* [2010b]. The upper (HSU) and lower (HSL) *Hashin and Shtrikman* [1962] bounds e.g. for the electrical permittivity of a mixture of two phases p_1 and p_2, with volumetric fraction (1- φ), φ and permittivity $\varepsilon_{p_2} > \varepsilon_{p_1}$ are given by

$$\varepsilon_{HSL}(\varepsilon_{p_1}, \varepsilon_{p_2}, \varphi) = \varepsilon_{p_1} + \frac{\varphi}{(\varepsilon_{p_2} - \varepsilon_{p_1})^{-1} + \frac{1-\varphi}{3\varepsilon_{p_1}}} \quad (1)$$

$$\varepsilon_{HSU}(\varepsilon_{p_1}, \varepsilon_{p_2}, \varphi) = \varepsilon_{p_2} + \frac{1-\varphi}{(\varepsilon_{p_1} - \varepsilon_{p_2})^{-1} + \frac{\varphi}{3\varepsilon_{p2}}}. \quad (2)$$

The model of *Brovelli and Cassiani* [2010b] relies on the assumption that at the pore level the porous medium can be approximated as a mixture of two components, with bulk properties corresponding to that of the upper and lower bound, respectively. In other words, within the porous material the water phase is locally well connected (and the bulk properties are computed from the upper HS bound), while in other regions where the fluid connectivity is lower the solid phase has stronger impact (and the bulk properties are computed from the lower HS bound). Ideally, one such system should be modeled using an effective medium approximation, using the HS bounds to compute the bulk properties of the two components. The resulting expression would however be extremely difficult to manipulate. The alternative approach followed by *Brovelli and Cassiani* [2010b] it so assume that the two components are arranged in parallel

rather than in a homogeneous isotropic mixture. The bulk permittivity of the assemblage, ε_b, is a linear combination of Equations (1) and (2):

$$\varepsilon_b = a\varepsilon_{HSU} + (1-a)\varepsilon_{HSL} \quad (3)$$

with the weighting factor, *a*, derived from *Archie*'s [1942] law, applied to dielectric properties:

$$\varepsilon_b = \frac{\varepsilon_p}{\phi^{-m}}. \quad (4)$$

Assuming that the (displacement) current flows primarily in the pore-fluid, i.e. that $\varepsilon_s/\varepsilon_p \to 0$, where ε_p is the permittity of the mixture that fills the pore space,

$$\varepsilon_b(\varepsilon_s, \varepsilon_p, \phi, m) = \left(\frac{3-\phi}{2}\phi^{(m-1)}\right)\varepsilon_{HSU}(\varepsilon_s, \varepsilon_p, \phi) + \left(1 + \frac{\phi-3}{2}\phi^{(m-1)}\right)\varepsilon_{HSL}(\varepsilon_s, \varepsilon_p, \phi), \quad (5)$$

where ϕ is porosity, *m* is Archie's cementation factor, ε_s is the permittivity of the mineral solid matrix and ε_p is the permittivity of the pore space. For 2-phase media, the permittivity of the pore-space is that of the fluid phase filling the pore space. More generally, for unsaturated materials, ε_p is given by the combination of the permittivity of 2 immiscible phases (water and non-aqueous phase) with $\varepsilon_w \gg \varepsilon_{NAPL}$,

$$\varepsilon_p(\varepsilon_w, \varepsilon_{NAPL}, s_w, n) = w\varepsilon_{HSU}(\varepsilon_w, \varepsilon_{NAPL}, s_w) + (1-w)\varepsilon_{HSL}(\varepsilon_w, \varepsilon_{NAPL}, s_w) \quad (6)$$

where ε_{NAPL} is the permittivity of the non-aqueous phase liquid (e.g. air or oil), s_w is water saturation ($0 \le s_w \le 1$) and *w* is a weight function, defined as:

$$w = \frac{\varepsilon_w}{\varepsilon_{HSU}(\varepsilon_w, 0, s_w)s_w^{-n}} \quad (7)$$

Owing to its derivation based upon Archie's law, the model of *Brovelli and Cassiani* [2010b] is applicable to geologic materials with negligible matrix and surface electrical conductance, that is, to sediments with negligible content of clays and metal oxides.

2.2 Surface conductance

According to *Revil and Glover* [1998] the conductance associated to the excess of charge at the water-matrix interface Σ_S is the sum of three components,

$$\Sigma_s = \int_0^\infty (\sigma(\chi) - \sigma_w) d\chi = \Sigma_s^S + \Sigma_s^D + \Sigma_s^H \ , \quad (8)$$

where Σ_s is the total surface conductance, σ_w is the electrical conductivity of the bulk fluid (i.e. far from the fluid-solid interface), $\sigma(\chi)$ the local electrical conductivity at a distance χ from the surface and $\Sigma_s^S, \Sigma_s^D, \Sigma_s^H$ are the conductances associated to the Stern and diffuse layers and to proton transfer at the interface, respectively. In natural conditions, the argument in the integral in Equation 8 vanishes at a distance of - at most - a few nanometers from the solid surface, a length scale named Debye length. *Microscopic* approaches [e.g. *Kan and Sen*, 1987; *Revil*, 1999; *Revil and Glover*, 1997; 1998; *Revil et al.*, 1998] were developed to compute the surface conductance of each component under simplified assumptions, in particular in presence of flat surfaces with uniform charge density and simple, well-defined pore water solutions. In reality, however, the identification of the parameters that characterize the surface of the skeleton is extremely difficult because the water-mineral interface is highly heterogeneous [*Adamson et al.*, 1966; *Van Riemsdijk et al.*, 1986]. In addition, the structure of the surface responds to changes in pore-fluid chemistry over a wide range of time scales. For this reason a *macroscopic* approach is often preferable, because it incorporates parameters that are more easily estimated on the basis of the composition and mineralogy of the medium (clay and organic matter content). According to one such model, the equivalent conductivity of the surface can be approximated as [*Kan and Sen*, 1987; *Revil and Glover*, 1998]:

$$\sigma_s = \frac{2}{3}\left(\frac{\phi}{1-\phi}\right)\beta_s Q_v = \frac{2}{3}\rho_m \beta_s CEC, \quad (9)$$

where β_s is the mobility of counterions in the EDL – the electrical double layer (the mobility in the EDL is lower than in the bulk fluid), Q_v is the excess surface charge per unit pore volume,

ρ_m is the density of the solid phase (grains) and *CEC* is the cation exchange capacity of the medium (in C kg^{-1} of solid matrix). One limitation of equation (9) is that it does not explicitly incorporate the dependence of surface conductivity on the ionic strength of the bulk solution. However, *Revil and Glover* [1998] tested Eq. (9) against the dataset of *Waxman and Smits* [1968]. They found that, within a realistic range of pore fluid concentration C_f ($C_f > 0.02$ mol l^{-1}), the surface conductivity in soils and geological formations is approximately a constant, and therefore the dependence of β_s and Q_v upon ionic strength can be neglected. The numerical model developed by *Brovelli and Cassiani* [2010a] was used to further confirm this result. The model solves numerically the coupled equations of electrokinetic flow in cylindrical geometries, and can be used to compute the bulk conductivity and electrokinetic coupling coefficients for 3D random networks of capillaries. It was observed that for natural fresh/brackish waters, that is, in the salinity range $0.02 \leq C_f \leq 0.5$ mol l^{-1}, both the Debye length and ζ-potential (the electrical potential of the Stern layer, a measure of the intensity of the EDL) decreased of about one order of magnitude. On the contrary, the bulk electrical conductivity scaled linearly with C_f, confirming the relative insensitivity of surface conductance to the ionic strength of the soil solution.

2.3 Extension of the *Brovelli and Cassiani* [2010b] model.

Using Eq. (9), surface conductance Σ_s can be converted into an equivalent volumetric conductivity σ_s. This approach is often referred to as the 'equivalent grain conductivity approach' [*Bussian*, 1983; *De Lima and Sharma*, 1990]. The surface conductance Σ_s and the volumetric conductivity σ_s are linked using a formula initially derived for charged macromolecules in aqueous solutions: $\sigma_S = 2\Sigma_S/\langle R \rangle$ [*O'Konski*, 1960], where $\langle R \rangle$ is a

224 characteristic length scale which for isolated smooth spherical particles corresponds to the radius
225 of the sphere. In soils and real porous media, the grains are often non-spherical, rough and show
226 a broad distribution of radii: in these conditions the median (or mean) grain size [*Brovelli et al.*,
227 2005; *Linde et al.*, 2006] or other characteristic lengths associated to the pores [e.g. *Johnson et*
228 *al.*, 1986] are used to approximate $\langle R \rangle$.

229 Using the grain conductivity approach, the model of *Brovelli and Cassiani* [2010b] can be
230 extended to represent porous media with non-negligible surface conductance. The electrical
231 conductivity component of the model can take a form analogous to the form for electrical
232 permittivity, thus making the model structure quasi-symmetric with respect to the two considered
233 electrical properties:

234 $$\sigma_b(\sigma_s, \sigma_p, \phi, m) = \left(\frac{3-\phi}{2}\phi^{(m-1)}\right)\sigma_{HSU}(\sigma_s, \sigma_p, \phi) + \left(1 + \frac{\phi-3}{2}\phi^{(m-1)}\right)\sigma_{HSL}(\sigma_s, \sigma_p, \phi), \quad (10)$$

235 The contribution of the pore-space electrical conductivity σ_p is computed by replacing the
236 permittivity of the water phase with the corresponding electrical conductivity in Equations (6)-
237 (7), while setting the electrical conductivity of the non-aqueous phase to 0. Under these
238 conditions, Equations (6)-(7) simplify to the second *Archie*'s [1942] law:

239 $$\sigma_p(\sigma_w, s_w, n) = \sigma_w s_w^n \quad (11)$$

240 In addition, as the magnitude of surface conductivity becomes negligible compared to that of the
241 bulk fluid (that is, as Dukhin number $\xi = \sigma_s/\sigma_w \to 0$) Eq. (10) reduces to the first *Archie*'s
242 [1942] law. Fig. 1 shows the variation of bulk electrical conductivity with increasing surface
243 conductivity (parameterized by ξ) and water saturation for different soil textures (the latter being
244 defined by porosity and Archie's cementation exponent *m*). The plots indicate that, at full
245 saturation, the bulk conductivity is modified by the contribution of the excess of charges at the
246 water/mineral interface only if $\xi >$ about 5×10^{-3}. Only in relatively dry soils ($s_w < 0.3$) with

247 low porosity the conductivity of the surfaces has a significant effect at small Dukhin numbers. In
248 soils with high porosity and low cementation exponent – that is, rounded grains and poor
249 cementation – the bulk conductivity is even less sensitive to surface conductivity. Only in very
250 dry conditions ($s_w < 0.15$), with fine texture, high specific surface area and high CEC (i.e.
251 $\xi > 10^{-2}$, see Eq. (9)) the excess of charge at the mineral/water interface alters significantly the
252 bulk electrical conductivity.
253 Eq. (10) together with Eqs. (1), (2), (6) and (9) provides a consistent framework to compute bulk
254 electrical conductivity and permittivity of variably saturated soils and other porous geological
255 formations. Owing to its derivation based upon a weighted average of the *Hashin and Shtrikman*
256 [1962] bounds, the constitutive model will be referred in the following to as the Hashin –
257 Shtrikman average (HSA) model.
258
259 **2.4 Other models for soil permittivity and electrical conductivity**
260 As noted in the introduction, some constitutive equations have already been proposed in
261 the literature, that use the same parameterization of Archie's laws to model the bulk electrical
262 conductivity of soils and shaly formations, where the contribution of the excess of charge at the
263 water-mineral interface cannot be neglected. These models can be used interchangeably for DC
264 conductivity and permittivity in the static limit. A specific objective of this work was to compare
265 our extended model with existing equations based on different assumptions, in order to ascertain
266 whether the different laws (and therefore the resulting calibrated parameters) could be used
267 interchangeably in soil mapping. The comparison was restricted to 2-phase mixtures, because
268 nearly all the equations for variably-saturated conditions reduce to $\sigma_b(s_w) = \sigma_b(s_w = 1)s_w^n$.
269 Many authors [e.g. *Brovelli et al.*, 2005; *Bussian*, 1983; *Clavier et al.*, 1984; *De Lima and*

Sharma, 1990; *Glover et al.*, 2000; *Waxman and Smits*, 1968] conceptualized the bulk electrical conductivity as made of two resistances in parallel, i.e.:

$$\sigma_b = f(\phi, m)\sigma_w + g(\phi, m)\sigma_s, \quad (12)$$

where $f(\cdot)$ and $g(\cdot)$ are two appropriate geometrical scaling factors, which depend only on the soil texture. Among these models, the best known and still widely employed is perhaps the equation proposed by *Waxman and Smits* [1968]:

$$\sigma_b = \frac{1}{F}(\sigma_w + \sigma_s), \quad (13)$$

where F is the formation factor ($F = \phi^{-m}$) and the surface conductivity σ_s given by Eq. (9). While Eq. (13) was developed based mainly on empirical evidences and a very simple conceptualization, a more physically sound methodology based on the volume averaging theorem was used by *Pride* [1994] to obtain a similar relationship, based on a two-parallel resistor parameterization:

$$\sigma_b = \frac{1}{F}[\sigma_w + (F-1)\sigma_s]. \quad (14)$$

This two-resistors in parallel approach is not entirely valid [for a discussion, see *Brovelli et al.*, 2005] because it neglects the interactions of current flow between surfaces and bulk fluid. In particular, Eq. (13) is not able to predict the existence of an isoelectric point [*Bolève et al.*, 2007] and of the non-linear behavior observed using pore solutions with low ionic strength: in these conditions the surface conductance dominates the bulk response of the medium ($\xi \to 1$ or larger).

Accurate predictions in the whole salinity range are better achieved using petrophysical models derived using effective medium approaches [*Bruggeman*, 1935; *Hanai*, 1960]. In particular the model of *Bussian* [1983]:

$$\sigma_b = \frac{\sigma_w}{F}\left(\frac{1-\xi}{1-\sigma_b/\sigma_s}\right)^m \quad (15)$$

was found to be often very accurate [*Bussian*, 1983; *Revil and Glover*, 1998]. In Eq. (15) the cementation factor m is related to *Bruggeman*′s [1935] depolarization factor, d as $m = 1/(1-d)$ and therefore m can be related to the geometry and assemblage of the grains. The main limitation of *Bussian's* [1983] law is that there is no exact explicit solution available. For this reason, *Revil and Glover* [1998] derived an approximate solution, assuming $m = 2$, a typical value for the cementation factor, that however show in practice a fairly large range. *Revil and Glover* [1998] also assumed that the electrical current in the EDL is only transported by cations, i.e. $t^f_{(-)} = 0$, where t^f stands for the Hittorf transport number of cations and anions (subscript + and -, respectively). As a consequence, *Revil and Glover* [1998] obtained:

$$\sigma_b = \frac{\sigma_w}{F}\left[1 - t^f_{(+)} + F\xi + \frac{1}{2}(t^f_{(+)} - \xi)\left(1 - \frac{\xi}{t^f_{(+)}} + \sqrt{\left(1 - \frac{\xi}{t^f_{(+)}}\right)^2 + 4F\frac{\xi}{t^f_{(+)}}}\right)\right]. \quad (14)$$

3. Results

3.1 Extended model validation against experimental data

Previous comparison of the *Brovelli and Cassiani* [2010b] model with electrical properties of clean porous media (for example sandy soils) and in conditions where the contribution of surface conductivity is negligible ($\xi \to 0$) suggested that the model is well suited to model the bulk electrical response of porous systems [*Brovelli and Cassiani*, 2010b]. The objective of this section is to verify whether the equivalent grain conductivity approach introduced in the HSA extended model allows it to be used satisfactorily in more general conditions. In particular, the points that need to be investigated are: (i) whether the model successfully reproduces

313 experimental data of clayey soils, and (ii) whether the resulting textural parameters –
314 cementation factor and saturation exponent – and the calibrated surface conductivity have
315 realistic values.

316 The comparison of the model against experimental data [from *Amente et al.*, 2000; *Binley*
317 *et al.*, 2002; *Doussan and Ruy*, 2009; *Friedman*, 1998; *Malicki and Walczak*, 1999; *Saarenketo*,
318 1998] is reported in Tables 1 and 2, and in Figures 2 to 4. Table 1 compares model predictions
319 with experimental data of soil bulk conductivity. The very high correlation coefficient (r^2)
320 indicates that the fit is excellent in practically all cases, and the calibrated parameters are
321 realistic. The datasets of *Amente et al.* [2000] and *Malicki and Walczak* [1999] were useful to
322 further verify the assumption that surface conductivity in field conditions is almost insensitive to
323 changes in pore-water salinity [*Revil and Glover*, 1998]. In these two datasets, the effective
324 conductivity of soil samples was measured as a function of water saturation using different pore-
325 solutions with increasing ionic strength. The HSA model was fitted simultaneously on all the
326 resulting curves, and we found that a unique set of parameters is able to reproduce the
327 experimental data of both sets. The surface conductivity obtained from the fitting is equal to
328 3.7×10^{-3} S/m and 1.2×10^{-2} S/m for the data of *Amente et al.* [2000] and *Malicki and Walczak*
329 [1999], respectively. It should however be noted that the values of pore-water conductivity
330 reported in *Malicki and Walczak* [1999] were not entirely realistic (for example, a conductivity
331 equal to 0 Sm^{-1} was reported, see caption of their Fig. 1). For this dataset the pore-water
332 conductivity was therefore corrected, since a de-ionized solution equilibrates very rapidly with
333 the soil. In other words, the electrical conductivity of the soil solution should have been
334 measured after the measurements. The two soils have moderate to high porosity, and the
335 cementation exponent is small. According to the above discussion (Fig. 1 and paragraph 2.3) for

such materials the model fitting is sensitive to surface conductivity only if $\xi > 5 \times 10^{-3}$. For both soils this condition is satisfied, and therefore the parameter obtained from the fitting procedure is meaningful. Fig. 2 compares model predictions for the shaly sandstone data of *Binley et al.* [2002]. The same dataset was also used by *Brovelli et al.* [2005] to test a pore-scale modeling tool developed to study the electrical properties of porous media. For this specific dataset, both electrical conductivity and permittivity measurements (as a function of saturation) were available, and they were fitted simultaneously. A satisfactory model fitting was achieved, and the obtained parameters were realistic. *Brovelli et al.* [2005] constructed a digital representation of the same geological material and used the digital sample to independently estimate the cementation exponent, obtaining a value $m \simeq 1.5$, which is compatible with, but slightly smaller than, the estimate from the HSA model fitting ($m \simeq 1.7$). A possible explanation for this discrepancy may be linked to the different shape of the soil grains in the real soil and its digital representation (the random packing of *Brovelli et al.* [2005] consisted of spherical particles). Fig. 3 compares the HSA model with the datasets of *Doussan and Ruy* [2009] consisting of Fontainbleau (clean) sand, a loam, and a silty clay loam. The fitting of the model is satisfactory for the sand and the loam, and the calibrated parameters (Table 1) are consistent with previous ranges reported in the literature [see e.g. *Lesmes and Friedman*, 2005]. On the contrary, for the silty clay loam the HSA model reproduced well only the data in the range of water saturation 0.0 – 0.7, whereas at higher values the measurements drift away with different slope. A possible explanation is that the soil has a dual porosity, with large pores in the intra-aggregate porosity and finer pores within the aggregates. The cementation exponent fits well the expected ranges from the literature, while the saturation exponent is higher than expected. This is consistent with the findings of *Brovelli and Cassiani* [2010b], who concluded that for dual

359 porosity materials $n > 4$ should be expected. The estimated surface conductivity for the samples
360 of *Doussan and Ruy* [2009] is negatively correlated with the mean grain diameter. D_{50} is equal to
361 256.3 μm, 31.8 μm and 6.8 μm for sand, loam and silty clay loam, respectively. The equivalent
362 surface conductivity can therefore be converted to surface conductance using the relationship
363 $\Sigma_s = \sigma_s \langle R \rangle / 2$ with $\langle R \rangle = 0.5 D_{50}$. The corresponding surface conductances are 3.2×10^{-9}S,
364 1.19×10^{-7}S and1.02×10^{-7} S for sand, loam and silty clay loam. These values are consistent with
365 previous findings [see a summary in *Brovelli et al.*, 2005]. Indeed, *Bolève et al.* [2007] criticized
366 the values reported in *Brovelli et al.* [2005] on the basis that triple layer calculations [*Leroy and*
367 *Revil*, 2004; *Revil and Glover*, 1997; *Revil et al.*, 1998] found that for all porous media $\Sigma_s \simeq$
368 5×10^{-9} S. A possible reason for the observed discrepancies is related to the identification of a
369 suitable length scale $\langle R \rangle$, as observed by *Bolève et al.* [2007]. A difference of about two orders of
370 magnitude (in terms of the estimated surface conductance) suggests that it may be not
371 appropriate to use the average grain size, at least for sediments having also a fine-grained soil
372 fraction, to estimate the equivalent surface conductivity. Note that, based on the surface
373 conductance estimate computed by *Revil and Glover* [1997] and others, *Linde et al.* [2006]
374 concluded that the grain size distribution of the same shaly sandstone considered by *Binley et al.*
375 [2002] must have had expected values in the 1 μm range, while in reality the Sherwood
376 Sandstone has a median grain size in the 200 μm range [see e.g. Fig.4 in *Binley et al.*, 2005].
377 Table 2 reports the comparison of the HSA model with bulk permittivity data for clayey
378 soils. The data of *Malicki and Walczak* [1999] (first row) were measured on the same soil sample
379 used for bulk conductivity measurements, and therefore the parameters were not estimated
380 independently from the permittivity data, but the values reported in Table 1 were used directly in
381 a predictive manner. Even without fitting parameters the HSA model compares well with the

382 experimental results (high r^2 in Table 2, plot not shown), indicating that parameters calibrated on
383 electrical conductivity can be used to estimate permittivity, and vice-versa. Fig. 4 visually
384 compares model predictions and laboratory measurements for the experimental data of
385 *Saarenketo*, [1998] (Houston black clay and Beaumont clay) and *Friedman*, [1998] (Sarid clay).
386 The model performed well with Sarid and the Houston black clays, whereas for the Beaumont
387 clay a lower correlation was found (despite the fact that the trend observed in the data was still
388 reproduced). This is likely an effect of the scatter in the experimental data. It was not a surprise
389 to find that experimental data for compact clays were noisy, since – owing to the changes
390 occurring in the sample when the moisture content is varied (for example, crack opening during
391 desiccation or swelling during imbibition) – drainage/imbibition experiments are normally more
392 difficult.
393
394 **3.2 Comparison with other petrophysical models**
395 Following successful validation with experimental data, the HSA model was compared
396 with the constitutive equations discussed in § 2.4 that use Archie's parameterization of the
397 porous medium. For the sake of simplicity, results are presented considering saturated conditions
398 only. Indeed, variably saturated conditions were also analyzed and the conclusions were similar
399 to those reached for two-phase systems. In all cases reported the cementation factor *m* was set to
400 2.5, but again this choice has no impact on the findings. The parameters that were varied and
401 analyzed were porosity and surface conductivity. Figure 5 compares the HSA model with the
402 constitutive equations of *Pride*, [1994] and *Waxman and Smits*, [1968]. The predictions with
403 *Pride*'s [1994] model closely reproduce those obtained with the HSA model if porosity is
404 moderate or large ($\phi > 0.25$) and the effect of surface conductivity is limited ($\xi < 10^{-2}$).

405 Outside these intervals the discrepancy between the two models increases, but indeed remains
406 only moderate (10% difference or less). Instead, the *Waxman and Smits*, [1968] model shows a
407 behavior compatible with the HSA model only as $\xi \rightarrow 0$, that is, when the two models reduce to
408 Archie's law. It can then be concluded that parameters estimated with the *Waxman and Smits*,
409 [1968] equation are not compatible with those obtained from the HSA model.
410 The equations developed by *Bussian*, [1983] and *Revil et al.*, [1998] are compared with the
411 HSA model in Fig. 6. Archie's law is also shown for comparison. For this comparison the
412 cementation exponent *m* was set to 2.5, and the cation Hittorf transport number ($t_{(+)}^{f}$) to 1 [e.g.
413 *Boléve et al.*, 2007]. *Revil and Glover* [1998] equation is however only slightly sensitive to this
414 parameter, and the comparison with the other two models is nearly unaffected by the value used.
415 The three models have nearly the same behavior, and the discrepancies remain very limited in
416 the entire porosity and surface conductivity ranges investigated. Quite surprisingly, although
417 developed on a completely different basis, the HSA and *Bussian* [1983] models show a
418 remarkably good agreement. It can therefore be concluded that the three models in Figure 6 can
419 be used interchangeably.
420

421 # 4. Mapping soil salinity

422 ### 4.1 Theory

423 Based on empirical observations, some previous studies [*Hamed et al.*, 2003; *Hilhorst*, 2000;
424 *Malicki and Walczak*, 1999] found that the relationship between bulk electrical conductivity and
425 bulk permittivity of variably saturated soil samples show a linear behavior for saturation larger
426 than about 20% (or bulk permittivity larger than 8). In other words, when electrical conductivity

427 and permittivity are measured simultaneously and cross-plotted, the resulting curve can be
428 parameterized as

429 $$\varepsilon_b = A\sigma_b + B \quad (15)$$

430 where A and B are empirical factors. This was explained by the fact that the two electrical
431 properties are affected by the water saturation changes in a similar way:

432 $$\frac{d\sigma_b}{ds_w} \simeq \frac{d\varepsilon_b}{ds_w}, \forall s_w > 0.2 \quad (16)$$

433 *Malicki and Walczak* [1999] and *Hilhorst et al*. [2000] observed that the slope A is sensitive
434 to changes in the conductivity of the pore-water, while the intercept B is affected by the soil
435 texture. For this reason, simultaneous measurements of DC conductivity and permittivity were
436 used to define a 'soil salinity index' [*Malicki and Walczak*, 1999]. To further develop this idea,
437 in this work we propose a closed-form relationship that allows the direct estimation of pore water
438 conductivity from simultaneous measurements of bulk conductivity and permittivity. To obtain
439 the sought relationship, two equations using the same parameterization of the soil electrical
440 response – one for electrical conductivity, the other for permittivity – were combined to give a
441 relationship of the form of Eq. (15). In saline soils, surface conductivity is negligible compared
442 to water conductivity ($\xi \to 0$), and bulk soil conductivity can be computed using the second
443 Archie's law:

444 $$\sigma_b = \frac{\sigma_w}{F} s_w^n \quad (17)$$

445 A possible equation that can model soil permittivity using the same parameterization as Archie's
446 law is the HSA model presented in section 2. The corresponding analytical expression is
447 however difficult to manipulate, and cannot be easily simplified to produce an analytical
448 expression that fits the observed linear behavior. An alternative approach to model permittivity is

449 to use the equation proposed by *Pride* [1994] which was extended to variably saturated
450 conditions by *Linde et al.*, [2006]:

451 $$\varepsilon_b = \frac{1}{F}[s_w^n \varepsilon_w + (1 - s_w^n)\varepsilon_a + (F - 1)\varepsilon_s] \quad (18)$$

452 Eq. (18) uses the same parameterization as Archie's law, and the influence of water saturation on
453 bulk permittivity is similar to that described by the HSA model – that is, $d\varepsilon_b^{PL}/ds_w \simeq$
454 $d\varepsilon_b^{HSA}/ds_w$, where ε_b^{PL} is the bulk conductivity obtained with the *Pride* [1994] and *Linde et al.*
455 [2006] equation and ε_b^{HSA} is the corresponding value computed with the HSA model – for wet
456 conditions ($s_w > 0.3$) and $\frac{\varepsilon_s}{\varepsilon_w} < 10^{-1}$ (see the comparison in *Brovelli and Cassiani* [2010b]).
457 Since the derivative $d\varepsilon_b/ds_w$ is what matters (Eq. 16), Eq. 17 and 18 can be combined – Eq.
458 (18) is written in terms of water saturation and it is replaced in Eq. (18) – to obtain a linear
459 relationship between conductivity and permittivity with slope:

460 $$A = \frac{\varepsilon_w - \varepsilon_a}{\sigma_w}, \quad (19)$$

461 and intercept:

462 $$B = \frac{\varepsilon_a}{F} + \frac{F-1}{F}\varepsilon_s. \quad (20)$$

463 where *A*, *B* are the parameters in Eq. 15, and *F* is the formation factor. The intercept *B* depends
464 on the texture of the soil and permittivity of the NAPL and solid matrix, while interestingly the
465 slope *A* is only affected by the properties of the mobile phases. *Hilhorst* [2000] studied the same
466 relationship and on the basis of empirical observations assumed $A = \varepsilon_w/\sigma_w$. This equation is
467 compatible with Eq. 19 in the case $\varepsilon_w \gg \varepsilon_a$, for example if the non wetting phase is air. For
468 other NAPLs with larger permittivity, Eq. 19 would be more accurate.
469 Since water and air relative permittivity values can be assumed as constants (80 and 1,
470 respectively), Eq. 19 can be directly used to map soil salinity (expressed in terms of electrical

conductivity of the pore water) from simultaneous measurements of bulk electrical conductivity and permittivity, with no adjustable parameter and without knowing the degree of water saturation. In practice, the bulk conductivity and permittivity of the soil (either in the laboratory or in the field) should be measured at least three times with different moisture content (that indeed can remain unknown), and a straight line must be fitted to the data. Eq. (19) is then used to convert the slope of the fitted line to pore-water electrical conductivity, assuming that such conductivity has not changed over time. In other words, model calibration in the laboratory is not necessary, and the estimation remains accurate regardless the lateral heterogeneity of the system and variations in lithology, soil texture and moisture content. The main limitation of the proposed approach is that during the measurement period the pore water electrical conductivity must remain approximately constant, that is, temperature changes and accumulation of salts in the topsoil, for example due to evaporation or plant water uptake, should be negligible.

4.2 Model verification

4.2.1 Procedure

To verify the findings above and validate the proposed methodology, we used a two-step approach. First, in order to verify the solidity of the introduced approximations – and in particular the fact that the model of *Pride* [1994] and *Linde et al.* [2006] was used – the results obtained using the linear approximation were compared with the predictions calculated using the more accurate variably saturated HSA model described above. The other aspect that needed to be addressed was the identification of the range of water saturation within which the linear approximation remains reliable. Previous experimental observations found that this limit is defined by a lower bulk relative permittivity ranging between 6 and 8 (in the following denoted

as ε_b^{min}) [*Hilhorst et al.*, 2000; *Persson*, 2002]. Second, we compared the predictions obtained using the linear approximation with some datasets where the bulk electrical properties (conductivity and permittivity) as well as the electrical conductivity of the pore water were independently measured. Results of the first part of the validation procedure are reported in Fig. 7 (black dots). The scatter plots compare the 'true' water conductivity with the results of the linear approximation. This value was computed fitting with a straight line a synthetic dataset composed of a number of pairs $(\varepsilon_b, \sigma_b)$ calculated using the HSA equation. The slope of the line was used to estimate water conductivity via Eq. (19), as discussed in the above paragraph. To evaluate the reliability of the linear approximation in the entire parameter space, a Monte Carlo procedure was adopted: 500 realizations were generated sampling the parameters from uniform distributions. The properties considered were porosity (in the range 0.15 to 0.50), pore-water conductivity ($10^{-3} \leq \sigma_w \leq 10$ S m^{-1}), cementation factor ($1.3 \leq m \leq 2.5$), saturation exponent ($1.3 \leq n \leq 2.5$) and matrix permittivity ($4.0 \leq \varepsilon_s \leq 7.5$). Two cases were studied: in the first ε_b^{min} was set to 7.5 (left panel of Fig. 7), in the second $\varepsilon_b^{min} = 10$ (Fig 7, right panel). In other words, only pairs $(\varepsilon_b, \sigma_b)$, with $\varepsilon_b \geq \varepsilon_b^{min}$ were used in the fitting.

The correlation between true and estimated parameters is very high regardless of the ε_b^{min} used, and raising the threshold from $\varepsilon_b^{min} = 7.5$ to $\varepsilon_b^{min} = 10$ resulted in a small but noticeable improvement, as indicated by the larger correlation coefficient (r^2in the figure). This suggests that the devised methodology provides better estimates if soils are moderately wet (that is, if $\varepsilon_b^{min} > 10$), Therefore we concluded that $\varepsilon_b^{min} = 8$ can be considered in general an appropriate threshold. The high correlation also confirms the validity of the assumptions made, including the use of the *Linde et al* [2006] equation to model bulk permittivity of variably saturated soils.

517 *4.2.2 Comparison with experimental data*

518 We further validated the methodology using experimental data [*Hamed et al.*, 2003; *Hilhorst*,
519 2000; *Malicki and Walczak*, 1999; *Persson*, 2002b]. The tested datasets cover a large range of
520 soil types and porous media: all estimated values are plotted in Fig. 7 (red squares, right panel)
521 and overall the comparison is remarkably good ($r^2 > 0.8$) despite the extreme simplicity of the
522 proposed relationship ($\varepsilon_w$was set to 80 in all cases). Table 3 reports the comparison for three
523 sets of data that are discussed in more detail in the following. Measurements performed on glass
524 beads [*Hilhorst*, 2000] and on an organic top soil [*Hamed et al.*, 2003] are plotted in Fig. 8 and
525 Fig. 9, respectively. The HSA model is shown for comparison on both plots, together with the
526 line fitted to the data to estimate the conductivity of the pore water. The estimated pore water
527 conductivity represents very well the measured value for both materials (Table 3) and bulk
528 permittivity increases linearly with conductivity, although for the organic top soil $\varepsilon_b^{min} \simeq 13$
529 (that is, only above this value the relationship is linear). This observation suggests that if
530 accurate results are sought, it may be appropriate to perform a preliminary laboratory study to
531 ascertain whether the relationship is effectively linear and to define a suitable ε_b^{min}. Fig. 8 and 9
532 also show the effect of surface conductivity (in terms of Dukhin number) on the relationship. The
533 interesting aspect is that the slope of the curve in wet conditions (defined by $\varepsilon_b > 15$) remains
534 approximately the same regardless the intensity of surface conductivity, and the main effect is a
535 shift of the curves towards higher conductivity values. In other words, these results indicate that
536 pore-water conductivity can be estimated using Eq. (19) regardless the value of surface
537 conductivity, provided that the soil is at least partly wet. A physical explanation for this
538 observation is that at moderate to high saturation values the bulk electrical conductivity remains
539 controlled by the conductivity of the pore fluid. This is consistent with the observations made in

Fig. 1, where it was observed that at $s_w > 0.5$ in natural conditions the electrical conductivity of materials with moderate to high porosity is only minimally affected by surface conductivity. It is therefore possible to conclude that in these conditions the linear approximation defined by Eq. (19) can be used to estimate water conductivity regardless the *CEC* of the medium.

The dataset of *Malicki and Walczak*, [1999] is reported in Fig. 10. The same data are also presented in §3.1 to test the applicability of the HSA model on soil electrical conductivity measurements. In §3.1 it was mentioned that the electrical conductivity of the pore fluid had to be adjusted to fit the data. This was done using the linear approximation presented in this section: each dataset was fitted with a straight line, and the conductivity computed via Eq. (19). The comparison reported in Table 3 shows that the estimated value predicted a higher electrical conductivity larger than that measured for the three solutions with lower ionic strength, while for the other two cases the match was satisfactory. This confirms the hypothesis made above that the electrical conductivity of the pore fluid changed once the ionic composition of the water equilibrated with the porous medium. The HSA model was fitted on the 5 datasets (same soil with different water conductivity) simultaneously. Quite unexpectedly the model reproduces the experimental data satisfactorily for three sets (with $r^2 \simeq 0.96$ or larger, open symbols in Fig. 10), while for the remainders the model under- and over-estimate the predictions. No clear explanation for this discrepancy was found.

5. Conclusions

The analysis conducted in this work indicated that bulk electrical conductivity and permittivity can be modeled using joint constitutive models. In particular, equations based on *Archie*'s [1942] parameterization of the soil properties (cementation and saturation exponents, *m* and *n*) proved suitable for this task. More specifically, in this work it was found that

- The equivalent grain conductivity approach introduced by *Bussian* [1983] can be used to include surface conductance in the computations of bulk soil conductivity, given that the couplings and interactions between conduction paths in the bulk fluid and at the mineral/water interface are correctly accounted for. This is true for non-linear models (such as that of *Bussian* [1983] and the HSA equation), but not for the 'two-resistors in parallel' type of models. This is consistent with previous findings of *Brovelli et al.* [2005] and *Bolève et al.* [2007], among others. One critical issue that remains open is how the equivalent grain (volumetric) conductivity can be translated into surface conductance, and vice-versa. Numerous experimental evidences suggest that the identification of the characteristic length scale $\langle R \rangle$ is difficult, in particular for medium- and fine-grained soil samples. This is an important aspect, and it needs to be investigated in detail in future studies. The extended HSA model was applied to several geological materials with non negligible surface conductance, and good agreement was found. The calibrated parameters were found to compare well with literature ranges.
- Among the tested models, three – the HSA model presented here, and those of *Bussian*, [1983] and *Revil and Glover* [1998] – predicted consistent results for the same soil type, saturation and ionic strength of the pore fluid. It should however be mentioned that the model of *Revil and Glover* [1998] is strictly applicable to electrical conductivity only (although an equivalent formulation for permittivity can be devised). These models can therefore be used in joint inversion/data fusion schemes, as they share the same parameterization and provide consistent predictions.
- The evaluation of soil salinity from simultaneous measurements of electrical conductivity and permittivity is an example of how the use of relationships based on the same parameterization

can be used to exploit the dependence of electrical properties on the same soil characteristics. The proposed methodology is simple and – at least based on the comparison with data conducted in this study – robust, in particular because no fitting parameter is needed and the procedure is not affected by heterogeneity and variation of soil properties. The main limitation is however that pore-water conductivity must remain approximately constant during the measurement period.

The key conclusion of this work was that electrical conductivity and permittivity of soils are affected in a similar way by texture, water saturation and characteristics of the mineral matrix and pore fluid. Therefore, the use of a consistent parameterization to study both properties can help in the identification of the characteristics of the soil, and reduce the uncertainty and sensitivity to measurement errors. To this end, the equations tested and validated in this study provide a suitable framework to study and estimate electrical properties of unsaturated soils.

6. Acknowledgements

This work was supported by the EU FP7 collaborative project iSOIL permittivity of soils soil related sciences – Linking geophysics, soil science and digital soil mapping". We acknowledge the constructive comments from A. Binley, S. Friedman and two anonymous reviewers.

References

Abdel Aal, G. Z., E. A. Atekwana, and L. D. Slater (2004), Effects of microbial processes on electrolytic and interfacial electrical properties of unconsolidated sediments, *Geophysical Research Letters*, *31*(12), L12505 12501-12504.

Adamson, A. W., I. Ling, L. Dormant, and M. Orem (1966), Physical adsorption on heterogeneous surfaces, *Journal of Colloid and Interface Science*, *21*(4), 445-457.

Amente, G., J. M. Baker, and C. F. Reece (2000), Estimation of soil solution electrical conductivity from bulk soil electrical conductivity in sandy soils, *Soil Science Society of America Journal*, *64*(6), 1931-1939.

Archie, G. E. (1942), The electrical resistivity log as an aid in determining some reservoir characteristics, *Trans. A.I.M.E.*, *146*, 54-62.

Atekwana, E. A. (2010), Geophysical signatures of microbial activity at hydrocarbon contaminated sites: A review, *Surveys in Geophysics*, *31*(2), 247-283.

Benderitter, Y., and J. J. Schott (1999), Short time variation of the resistivity in an unsaturated soil: The relationship with rainfall, *European Journal of Environmental and Engineering Geophysics*, *4*(1), 37-49.

Binley, A., P. Winship, R. Middleton, M. Pokar, and J. West (2001), High-resolution characterization of vadose zone dynamics using cross-borehole radar, *Water Resources Research*, *37*(11), 2639-2652.

Binley, A., P. Winship, L. J. West, M. Pokar, and R. Middleton (2002), Seasonal variation of moisture content in unsaturated sandstone inferred from borehole radar and resistivity profiles, *Journal of Hydrology*, *267*(3-4), 160-172.

Binley, A.M., L.D. Slater, M. Fukes, and G. Cassiani (2005), The relationship between

627 frequency dependent electrical resistivity and hydraulic properties of saturated and
628 unsaturated sandstone, *Water Resources Research*, *41*(12), W12417
629 http://dx.doi.org/10.1029/2005WR004202.
630 Birchak, J.R., C.G. Gardner, J.E. Hipp, and J.M. Victor, (1974), High dielectric constant
631 microwave probes for sensing soil moisture, *Proc. IEEE,* **62**(1), 93–98.
632 Bolève, A., A. Crespy, A. Revil, F. Janod, and J. L. Mattiuzzo (2007), Streaming potentials of
633 granular media: Influence of the Dukhin and Reynolds numbers, *J. Geophys. Res.*, *112*(B8),
634 B08204.
635 Brovelli, A., and G. Cassiani (2008), Effective permittivity of porous media: A critical analysis
636 of the complex refractive index model, *Geophysical Prospecting*, *56*(5), 715-727.
637 Brovelli, A., and G. Cassiani (2010a), Sensitivity of Intrinsic Permeability to Electrokinetic
638 Coupling in Shaly and Clayey Porous Media, *Transport in Porous Media*, *83*(3), 681-697.
639 Brovelli, A., and G. Cassiani (2010b), A combination of the Hashin-Shtrikman bounds aimed at
640 modelling electrical conductivity and permittivity of variably saturated porous media,
641 *Geophysical Journal International*, *180*(1), 225-237.
642 Brovelli, A., G. Cassiani, E. Dalla, F. Bergamini, D. Pitea, and A. M. Binley (2005), Electrical
643 properties of partially saturated sandstones: Novel computational approach with
644 hydrogeophysical applications, *Water Resources Research*, *41*(8), W08411,
645 doi:10.1029/2004WR003628.
646 Bruggeman, D. A. G. (1935), Berechnung verschiedener physikalischer Konstanten von
647 heterogenen Substanzen. I. Dielektrizitätskonstanten und Leitfähigkeiten der Mischkörper aus
648 isotropen Substanzen, *Annalen der Physik*, *416*(7), 636-664.
649 Bussian, A. E. (1983), Electrical conductance in a porous medium, *Geophysics*, *48*(9), 1258-

650 1268.
651 Cassiani, G., V. Bruno, A. Villa, N. Fusi, A.M. Binley (2006), A saline tracer test monitored via
652 time-lapse surface electrical resistivity tomography, *Journal of Applied Geophysics*, 59, 244-
653 259.
654 Cassiani, G., A. Godio, S. Stocco, A. Villa, R. Deiana, P. Frattini, and M. Rossi (2009),
655 Monitoring the hydrologic behaviour of a mountain slope via time-lapse electrical resistivity
656 tomography, *Near Surface Geophysics*, *7*(5-6), 475-486.
657 Chen, Y., and D. Or (2006), Geometrical factors and interfacial processes affecting complex
658 dielectric permittivity of partially saturated porous media, *Water Resources Research, 42*(6),
659 W06423, doi:10.1029/2005WR004744.
660 Clavier, C., G. Coates, and J. Dumanoir (1984), Theoretical and experimental bases for the dual-
661 water model for the interpretation of shaly sands, *Society of Petroleum Engineers Journal*,
662 *24*(2), 153-168.
663 Corwin D.L., S.R. Kaffka, J.W. Hopmans, Y. Mori, J.W. van Groenigen, C. van Kessel, S.M.
664 Lesch and J.D. Oster (2003), Assessment and field-scale mapping of soil quality properties of
665 a saline-sodic soil, *Geoderma*, 114, 231– 259.
666 Corwin D.L. and S.M. Lesch (2005a), Characterizing soil spatial variability with apparent soil
667 electrical conductivity, I. Survey protocols, *Computers and Electronics in Agriculture*, 46,
668 103–133.
669 Corwin D.L. and S.M. Lesch (2005b), Characterizing soil spatial variability with apparent soil
670 electrical conductivity, Part II. Case study, *Computers and Electronics in Agriculture*, 46,
671 135–152.
672 Dannowski, G., and U. Yaramanci (1999), Estimation of water content and porosity using

673 combined radar and geoelectrical measurements, *European Journal of Environmental and*
674 *Engineering Geophysics*, *4*(1), 71-85.
675 Day-Lewis, F. D., and K. Singha (2008), Geoelectrical inference of mass transfer parameters
676 using temporal moments, *Water Resources Research*, *44*(5), W05201,
677 doi:10.1029/2007WR006750
678 Day-Lewis, F. D., K. Singha, and A. M. Binley (2005), Applying petrophysical models to radar
679 travel time and electrical resistivity tomograms: Resolution-dependent limitations, *Journal of*
680 *Geophysical Research B: Solid Earth*, *110*(8), 1-17.
681 De Lima, O. A. L., and M. M. Sharma (1990), A grain conductivity approach to shaly
682 sandstones, *Geophysics*, *55*(10), 1347-1356.
683 Doussan, C., and S. Ruy (2009), Prediction of unsaturated soil hydraulic conductivity with
684 electrical conductivity, *Water Resources Research*, *45*(10), W10408,
685 doi:10.1029/2008WR007309
686 Friedman, S. P. (1998), A saturation degree-dependent composite spheres model for describing
687 the effective dielectric constant of unsaturated porous media, *Water Resources Research*,
688 *34*(11), 2949-2961.
689 Friedman, S. P. (2005), Soil properties influencing apparent electrical conductivity: A review,
690 *Computers and Electronics in Agriculture*, *46*(1-3), 45-70.
691 Gallardo, L. A., and M. A. Meju (2004), Joint two-dimensional DC resistivity and seismic travel
692 time inversion with cross-gradients constraints, *Journal of Geophysical Research B: Solid*
693 *Earth*, *109*(3), B03311, 1-11.
694 Glover, P. W. J., M. J. Hole, and J. Pous (2000), A modified Archie's law for two conducting
695 phases, *Earth and Planetary Science Letters*, *180*(3-4), 369-383.

696 Haber, E., and D. Oldenburg (1997), Joint inversion: A structural approach, *Inverse Problems*,
697 *13*(1), 63-77.
698 Hamed, Y., M. Persson, and R. Berndtsson (2003), Soil solution electrical conductivity
699 measurements using different dielectric techniques, *Soil Science Society of America Journal*,
700 *67*(4), 1071-1078.
701 Hanai, T. (1960), Theory of the dielectric dispersion due to the interfacial polarization and its
702 application to emulsions, *Colloid & Polymer Science*, *171*(1), 23-31.
703 Hashin, Z., and S. Shtrikman (1962), A Variational approach to the theory of the effective
704 magnetic permeability of multiphase materials, *Journal of Applied Physics*, *33*(10), 3125-
705 3131.
706 Hayley, K., L. R. Bentley, and M. Gharibi (2009), Time-lapse electrical resistivity monitoring of
707 salt-affected soil and groundwater, *Water Resources Research*, *45*(7), W07425,
708 doi:10.1029/2008WR007616
709 Hilhorst, M. A. (2000), A pore water conductivity sensor, *Soil Science Society of America*
710 *Journal*, *64*(6), 1922-1925.
711 Hinnell, A. C., T. P. A. Ferré, J. A. Vrugt, J. A. Huisman, S. Moysey, J. Rings, and M. B.
712 Kowalsky (2010), Improved extraction of hydrologic information from geophysical data
713 through coupled hydrogeophysical inversion, *Water Resources Research*, *46*(4), W00D40,
714 doi:10.1029/2008WR007060
715 Hubbard, S. S., J. Chen, J. Peterson, E. L. Majer, K. H. Williams, D. J. Swift, B. Mailloux, and
716 Y. Rubin (2001), Hydrogeological characterization of the South Oyster bacterial transport site
717 using geophysical data, *Water Resources Research*, *37*(10), 2431-2456.
718 Huisman J.A., S. S. Hubbard, J. D. Redman, and A. P. Annan (2003), Measuring soil water

719 content with ground penetrating radar: A review, *Vadose Zone Journal 2*(4), 476–491.
720 Johnson, D. L., J. Koplik, and L. M. Schwartz (1986), New pore-size parameter characterizing
721 transport in porous media, *Physical Review Letters*, *57*(20), 2564-2567.
722 Kan, R., and P. N. Sen (1987), Electrolytic conduction in periodic arrays of insulators with
723 charges, *The Journal of Chemical Physics*, *86*(10), 5748-5756.
724 Kästner, M., and G. Cassiani (2009), ModelPROBE: Model driven soil probing, site assessment
725 and evaluation, *Reviews in Environmental Science and Biotechnology*, *8*(2), 131-136.
726 Knight, R., and A. Abad (1995), Rock/water interaction in dielectric properties: experiments
727 with hydrophobic sandstones, *Geophysics*, *60*(2), 431-436.
728 Koestel, J., A. Kemna, M. Javaux, A. Binley, and H. Vereecken (2008), Quantitative imaging of
729 solute transport in an unsaturated and undisturbed soil monolith with 3-D ERT and TDR,
730 *Water Resources Research*, *44*(12), W12411, doi:10.1029/2007WR006755
731 Koestel, J., J. Vanderborght, M. Javaux, A. Kemna, A. Binley, and H. Vereecken (2009a),
732 Noninvasive 3-D transport characterization in a sandy soil using ERT: 1. investigating the
733 validity of ERT-derived transport parameters, *Vadose Zone Journal*, *8*(3), 711-722.
734 Koestel, J., R. Kasteel, A. Kemna, O. Esser, M. Javaux, A. Binley, and H. Vereecken (2009b),
735 Imaging brilliant blue stained soil by means of electrical resistivity tomography, *Vadose Zone*
736 *Journal*, *8*(4), 963-975.
737 Leroy, P., and A. Revil (2004), A triple-layer model of the surface electrochemical properties of
738 clay minerals, *Journal of Colloid and Interface Science*, *270*(2), 371-380.
739 Lesmes, D and S. Friedman (2005) Electrical and hydrogeological properties. In Rubin, Y., and
740 S. S. Hubbard Eds., *Hydrogeophysics*, Springer, The Netherlands; 523 pp.
741 Linde, N., A. Binley, A. Tryggvason, L. B. Pedersen, and A. Revil (2006), Improved

742 hydrogeophysical characterization using joint inversion of cross-hole electrical resistance and
743 ground-penetrating radar traveltime data, *Water Resources Research*, *42*(12), W12404,
744 doi:10.1029/2006WR005131
745 Looms, M. C., A. Binley, K. H. Jensen, L. Nielsen, and T. M. Hansen (2008), Identifying
746 unsaturated hydraulic parameters using an integrated data fusion approach on cross-borehole
747 geophysical data, *Vadose Zone Journal*, *7*(1), 238-248.
748 Malicki, M. A., and R. T. Walczak (1999), Evaluating soil salinity status from bulk electrical
749 conductivity and permittivity, *European Journal of Soil Science*, *50*(3), 505-514.
750 Miller, M. N. (1969), Bounds for effective electrical, thermal, and magnetic properties of
751 heterogeneous materials, *Journal of Mathematical Physics*, *10*(11), 1988-2004.
752 Milton, G. W. (1981), Bounds on the electromagnetic, elastic, and other properties of two-
753 component composites, *Physical Review Letters*, *46*(8), 542-545.
754 Müller, K., J. Vanderborght, A. Englert, A. Kemna, J. A. Huisman, J. Rings, and H. Vereecken
755 (2010), Imaging and characterization of solute transport during two tracer tests in a shallow
756 aquifer using electrical resistivity tomography and multilevel groundwater samplers, *Water*
757 *Resources Research*, *46*(3), W03502, doi:10.1029/2008WR007595
758 O'Konski, C. T. (1960), Electric properties of macromolecules. V. Theory of ionic polarization in
759 polyelectrolytes, *Journal of Physical Chemistry*, *64*(5), 605-619.
760 Persson, M. (2002), Evaluating the linear dielectric constant - electrical conductivity model using
761 time-domain reflectometry, *Hydrological Sciences Journal*, *47*(2), 269-277.
762 Pride, S. (1994), Governing equations for the coupled electromagnetics and acoustics of porous
763 media, *Physical Review B*, *50*(21), 15678-15696.
764 Revil, A. (1999), Ionic diffusivity, electrical conductivity, membrane and thermoelectric

765 potentials in colloids and granular porous media: A unified model, *Journal of Colloid and*
766 *Interface Science*, *212*(2), 503-522.
767 Revil, A., and P. W. J. Glover (1997), Theory of ionic-surface electrical conduction in porous
768 media, *Physical Review B - Condensed Matter and Materials Physics*, *55*(3), 1757-1773.
769 Revil, A., and P. W. J. Glover (1998), Nature of surface electrical conductivity in natural sands,
770 sandstones, and clays, *Geophysical Research Letters*, *25*(5), 691-694.
771 Revil, A., L. M. Cathles, S. Losh, and J. A. Nunn (1998), Electrical conductivity in shaly sands
772 with geophysical applications, *Journal of Geophysical Research B: Solid Earth*, *103*(10),
773 23925-23936.
774 Rings, J., J. A. Huisman, and H. Vereecken (2010), Coupled hydrogeophysical parameter
775 estimation using a sequential Bayesian approach, *Hydrology and Earth System Sciences*,
776 *14*(3), 545-556.
777 Robinson, D. A., and S. P. Friedman (2001), Effect of particle size distribution on the effective
778 dielectric permittivity of saturated granular media, *Water Resources Research*, *37*(1), 33-40.
779 Robinson D.A., S. B. Jones, J. M. Wraith, D. Or, and S. P. Friedman (2003), A review of
780 advances in dielectric and electrical conductivity measurement in soils using time domain
781 reflectometry, *Vadose Zone Journal 2*(4), 444–475.
782 Roth, K., R. Schulin, H. Fluhler, and W. Attinger (1990), Calibration of time domain
783 reflectometry for water content measurement using a composite dielectric approach, *Water*
784 *Resources Research*, *26*(10), 2267-2273.
785 Rubin, Y., and S. S. Hubbard (2005), *Hydrogeophysics*, Springer, Dordrecht Netherlands; New
786 York. 523 pp.
787 Saarenketo, T. (1998), Electrical properties of water in clay and silty soils, *Journal of Applied*

788 *Geophysics*, *40*(1-3), 73-88.
789 Schwartz, B. F., M. E. Schreiber, and T. Yan (2008), Quantifying field-scale soil moisture using
790 electrical resistivity imaging, *Journal of Hydrology*, *362*(3-4), 234-246.
791 Sen, C., P. N. Scala, and M. H. Cohen (1981), A self-similar model for sedimentary rocks with
792 application to the dielectric constant of fused glass beads, *Geophysics*, *46*(5), 781-795.
793 Shevnin, V., A. Mousatov, A. Ryjov, and O. Delgado-rodriquez (2007), Estimation of clay
794 content in soil based on resistivity modelling and laboratory measurements, *Geophysical*
795 *Prospecting*, *55*(2), 265-275.
796 Suman, R. J., and R. J. Knight (1997), Effects of pore structure and wettability on the electrical
797 resistivity of partially saturated rocks - A network study, *Geophysics*, *62*(4), 1151-1162.
798 Topp, G. C., J. L. Davis, and A. P. Annan (1980), Electromagnetic determination of soil water
799 content: measurements in coaxial transmission lines, *Water Resources Research*, *16*(3), 574-
800 582.
801 Van Riemsdijk, W. H., G. H. Bolt, L. K. Koopal, and J. Blaakmeer (1986), Electrolyte
802 adsorption on heterogeneous surfaces: adsorption models, *Journal of Colloid and Interface*
803 *Science*, *109*(1), 219-228.
804 Vereecken H., A. Binley, G. Cassiani, I. Kharkhordin, A. Revil, K. Titov (2006), Applied
805 Hydrogeophysics, Springer-Verlag, Berlin, 383 pp.
806 Vozoff, K., and D. L. B. Jupp (1975), Joint Inversion of Geophysical Data, *Geophysical Journal*
807 *of the Royal Astronomical Society*, *42*(3), 977-991.
808 Waxman, M. H., and L. J. M. Smits (1968), Electrical conductivities in oil-bearing shaly sands,
809 *Soc. Petr. Eng. J.*, *8*, 107-122.
810

Tables

Table 1. Model testing using electrical conductivity of variably saturated soils: fitted parameters and correlation coefficients. Surface conductivity, cementation exponent *m* and saturation exponent *n* have been calibrated against lab data. See also Figures 2 and 3 for the fitting curves.

Soil type	Conductivity (S m^{-1})		Textural parameters			r^2	Reference
	pore-water	surface	ϕ	*m*	*n*		
Sandy loam	0.10	3.7×10^{-3}	0.38	1.68	1.8	> 0.999	[*Amente et al.*, 2000]
	0.15					> 0.999	
	0.21					> 0.999	
	0.24					> 0.999	
	0.30					0.999	
	0.37					0.998	
	0.40					> 0.999	
	0.56					0.999	
Sandy loam(1)	1.64×10^{-1}	1.2×10^{-2}	0.49	1.4	2.4	0.982	[*Malicki and Walczak*, 1999]
	1.93×10^{-1}					0.926	
	5.49×10^{-1}					0.988	
	7.87×10^{-1}					0.996	
	1.13					0.999	
Shaly sandstone	6.8×10^{-2}	2.5×10^{-3}	0.39	1.7	2.0	0.992	[*Binley et al.*, 2002]
Sand	6.5×10^{-2}	5×10^{-5}	0.36	1.3	1.8	0.989	[*Doussan and Ruy*, 2009]
Loam	7.14×10^{-2}	1.5×10^{-2}	0.44	1.3	1.9	0.994	
Silty clay loam	7.14×10^{-2}	6×10^{-2}	0.38	1.5	11	0.919	

(1) The conductivity of the pore-water reported in the original publication for this dataset had to be slightly modified. See text for explanations.

818

819 **Table 2.** Application of the proposed constitutive equation to model the permittivity of variably
820 saturated soils. Solid matrix permittivity, cementation factor *m* and saturation exponent *n* have
821 been calibrated against lab data. Water permittivity was set to 80 for all samples. See also
822 Figures 2 and 4 for the fitting curves.

Soil type	ω MHz	Matrix permittivity	Textural parameters ϕ	$m^{(1)}$	$n^{(1)}$	r^2	Reference
Sandy loam	TDR	5.5	0.49	1.4	2.4	0.998	[*Malicki and Walczak*, 1999]
Shaly sandstone	500	6.0	0.39	1.7	2.0	0.992	[*Binley et al.*, 2002]
	300					0.969	
Vertisol		6.5	0.62	2.2	2.5	0.998	[*Friedman*, 1998]
Houston black clay	500	6.5	0.45	2.6	2.5	0.974	[*Saarenketo*, 1998]
Beaumont clay	500	10.5	0.5	2.5	2.5	0.919	[*Saarenketo*, 1998]

823

824 **Table 3.** Measured conductivity of the pore water and comparison with the estimated values
825 using the linear approximation method presented in this paper. Additional experimental data are
826 reported in Fig. 7 (red squares). The comparison for the dataset of *Malicki and Walczak*, [1999]
827 is not fully satisfactory, as discussed in the text.

Soil type	Range	Pore-water conductivity [S m^{-1}]		Reference
		Measured	Estimated	
Glass beads	ε_b^{min}>10	0.4	0.42	[*Hilhorst*, 2000]
Top soil (organic)	ε_b^{min}>13	2.9×10^{-3}	2.63×10^{-3}	[*Hamed et al.*, 2003]
Silty loam	ε_b^{min}>10	0.0	1.64×10^{-1}	[*Malicki and Walczak*, 1999]
		1.27×10^{-1}	1.93×10^{-1}	
		3.88×10^{-1}	5.49×10^{-1}	
		8.25×10^{-1}	7.87×10^{-1}	
		1.17	1.13	

Figures

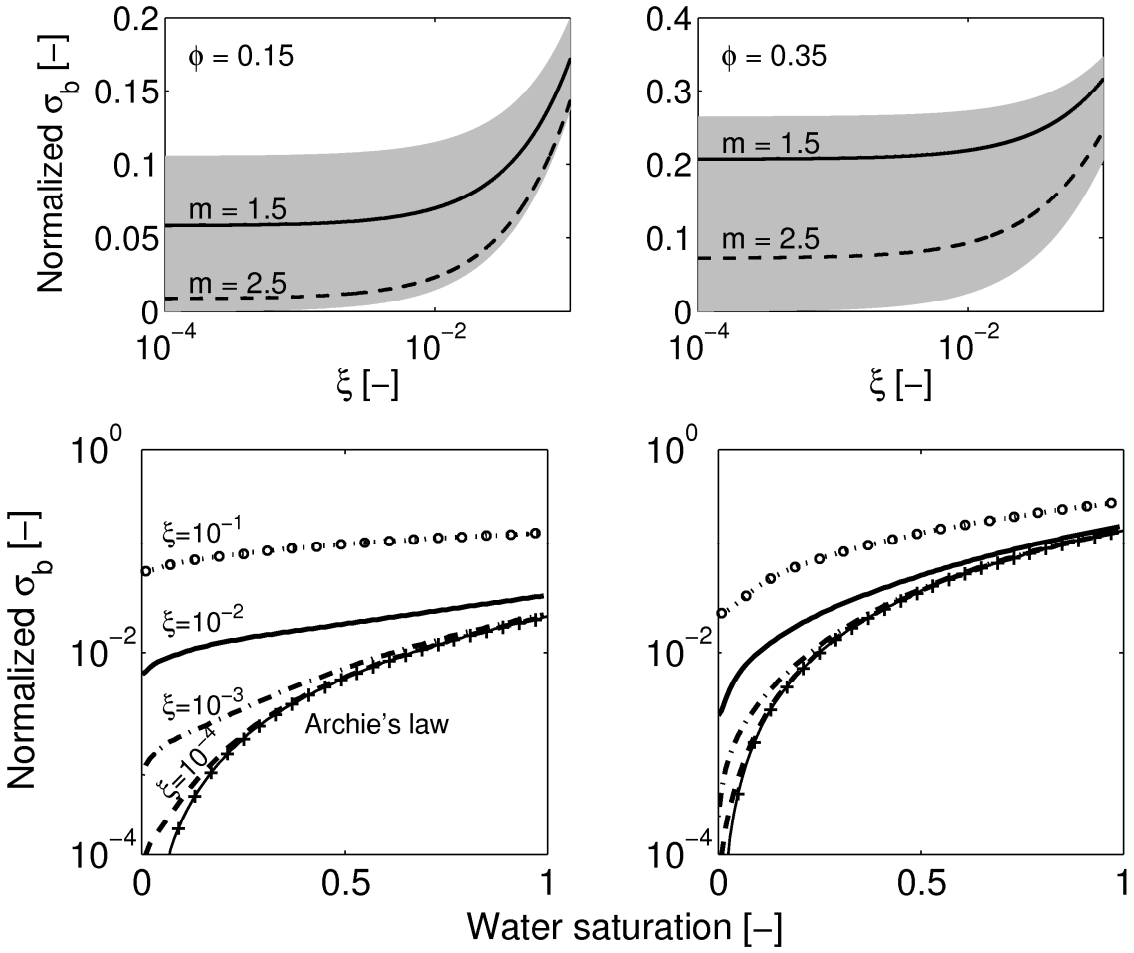

Figure 1. Bulk DC electrical conductivity according to the extended constitutive model based on *Brovelli and Cassiani* [2010b] as a function of the Dukhin number ξ. The model behavior is shown for fully saturated conditions (top panels) and variably saturated conditions (bottom panels). The area shaded in gray defines the possible range of variation of the bulk properties according to the *Hashin and Shtrikman* [1962] bounds.

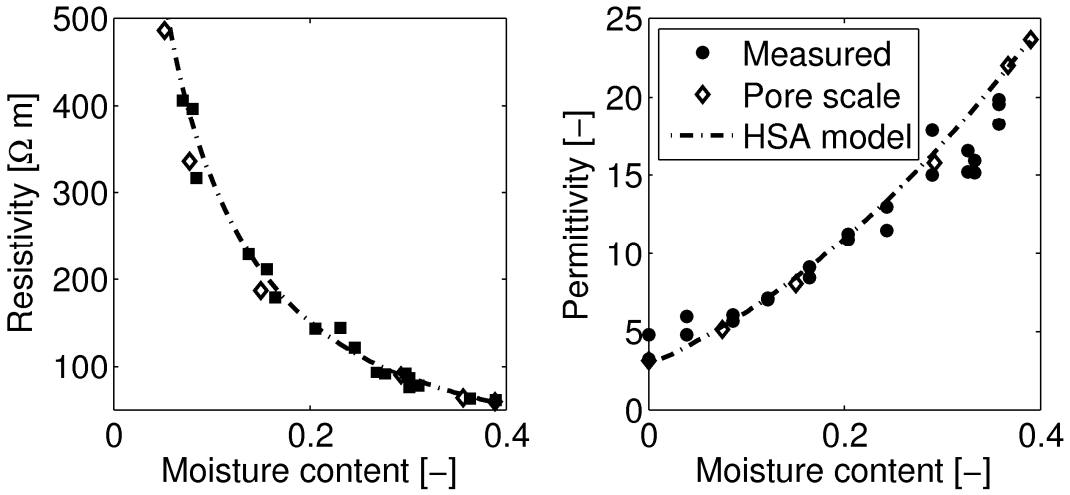

837

838

839 **Figure 2.** Comparison of the constitutive equation presented in this work with bulk electrical
840 resistivity and permittivity data taken from pore-scale modelling results (open diamonds, *Brovelli et*
841 *al.* [2005]) and experimental data *Binley et al.* [2002] for a shaly sandstone. Model parameters and
842 correlation coefficients are reported in Table 1 (electrical conductivity) and Table 2 (permittivity).

843

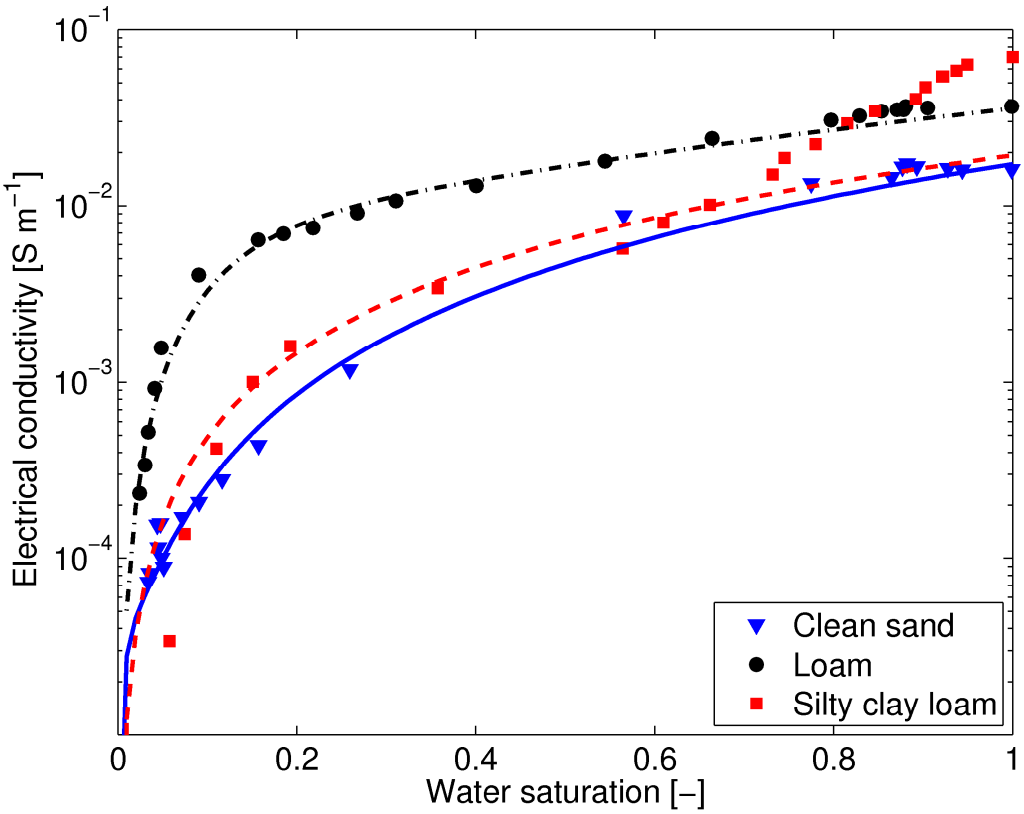

844

845 **Figure 3. V**alidation of the HSA equation using experimental data of three variably-saturated soils
846 with different texture [*Doussan and Ruy*, 2009]: sand (negligible surface conductivity), loam and
847 silty clay loam. Model parameters and correlation coefficients are listed in Table 1. While for the
848 sandy and loamy soils the comparison is satisfactory in the entire range of saturation, for the clayey
849 material the model fails to predict the increase in conductivity at saturation larger than 0.75.

850

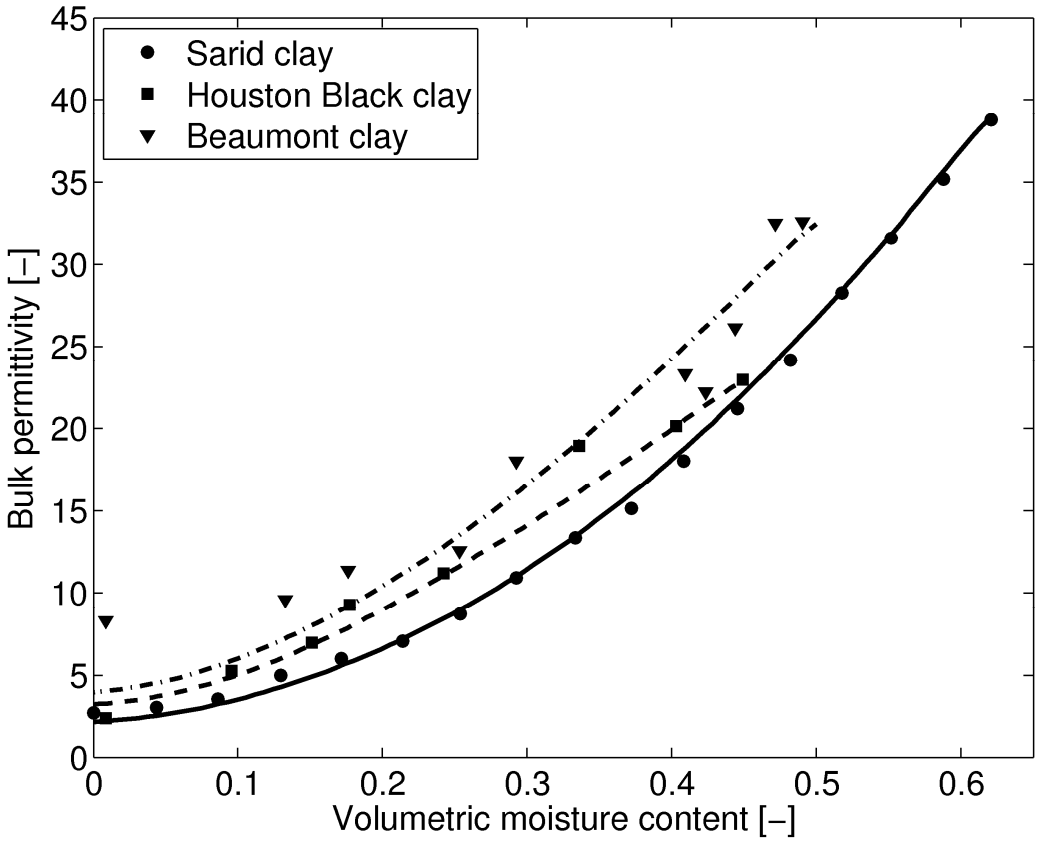

851

852 **Figure 4.** Model validation for the permittivity of variably saturated clayey soils [*Friedman*, 1998;
853 *Saarenketo*, 1998]. The comparison is overall satisfactory, although for one case (Beaumont clay)
854 the model under-predicts the permittivity at low water content ( ).This might be due to
855 changes in the geometry of the solid phase in dry conditions (for example, formation of cracks).

856

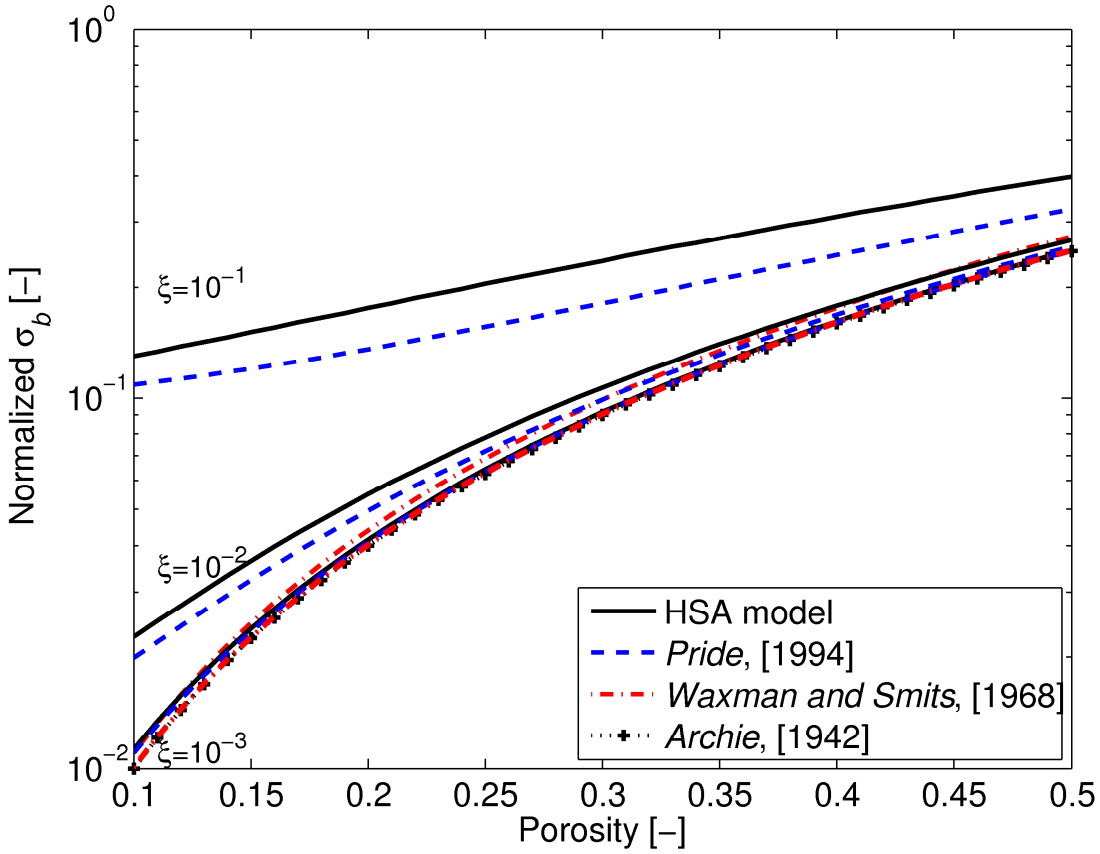

857

858 **Figure 5.** Comparison of the HSA model with the relationships of *Waxman and Smits* [1968] and of
859 *Pride* [1994]. *Archie*'s [1942] law is also reported for comparison. The cementation factor was set
860 to 2.5. The bulk conductivity was normalized using the electrical conductivity of the pore-water.
861 The proposed model does not reproduce the behavior of the Waxman and Smits equation, and
862 agrees well with the *Pride* [1994] relationship only when the surface conductance is low. The
863 *Waxman and Smits* [1968] model is only slightly sensitive to changes in surface conductance, and
864 the curves of this model for different ξ are almost overlapping.

865

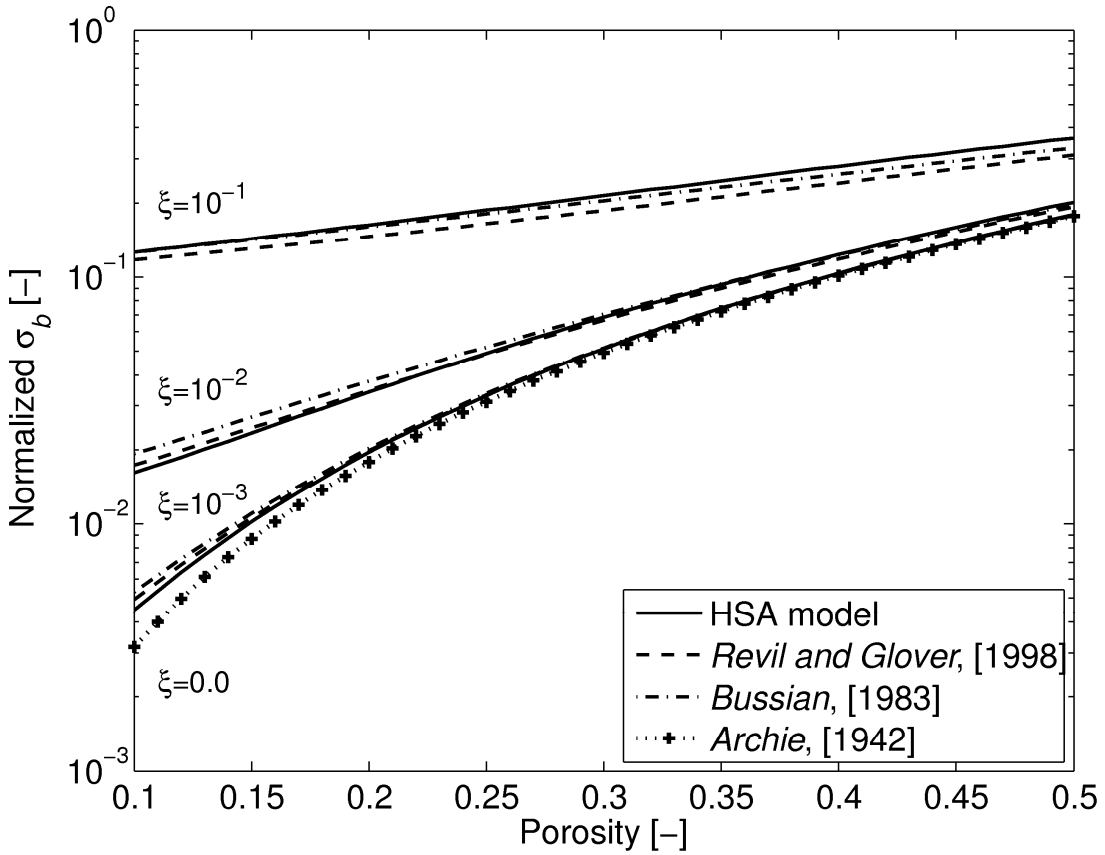

866

867 **Figure 6.** Comparison of the HSA model for a range of surface conductivities with the models of
868 *Bussian* [1983] and *Revil and Glover* [1998]. The three models share the same parameterization,
869 and reduce to *Archie*'s [1942] law when the electrical conductivity of the pore-fluid is much greater
870 than the surface conductance ($\xi \to 0$).

871

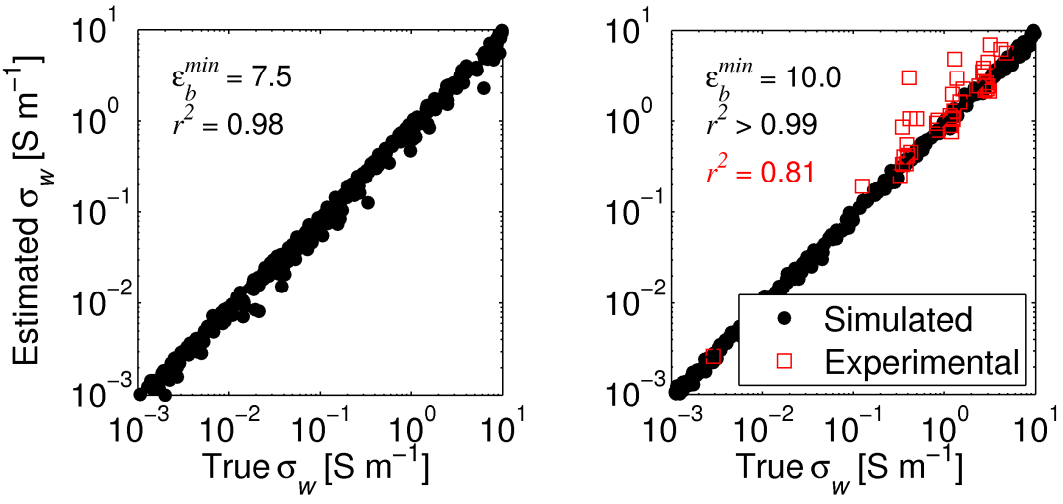

872

873 **Figure 7.** Estimated pore water conductivity using the linear approximation discussed in the text.
874 The constitutive model presented in this work was used to generate synthetic datasets of bulk
875 electrical conductivity and permittivity for different types of soils as a function of water saturation.
876 The estimated values compare well with the 'true' values, suggesting that the simplifications
877 introduced do not affect significantly the accuracy of the model.

878

879

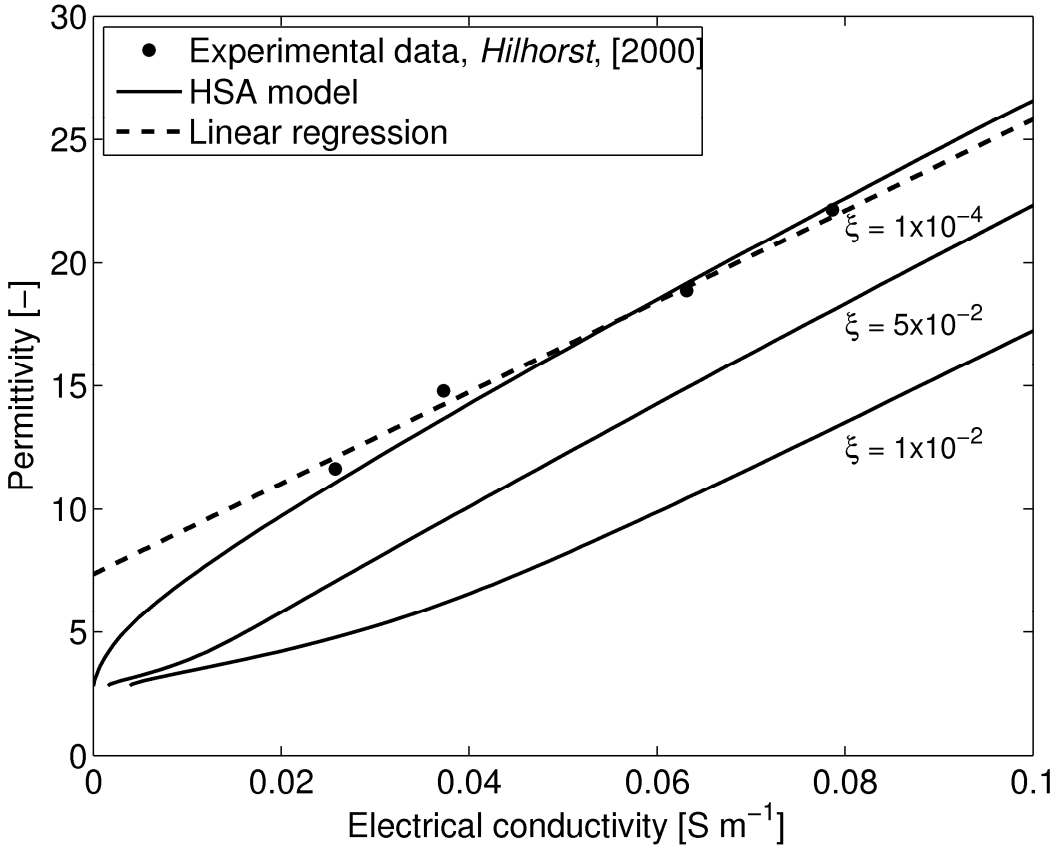

880

881 **Figure 8.** Permittivity versus electrical conductivity relationship for glass beads. Data from
882 *Hilhorst*, [2000]. The dashed line shows the linear regression of the experimental data. Using Eq.
883 (19) water electrical conductivity was estimated, and the result (0.42 Sm^{-1}) compares well with the
884 measured value (0.4 S m^{-1}).

885

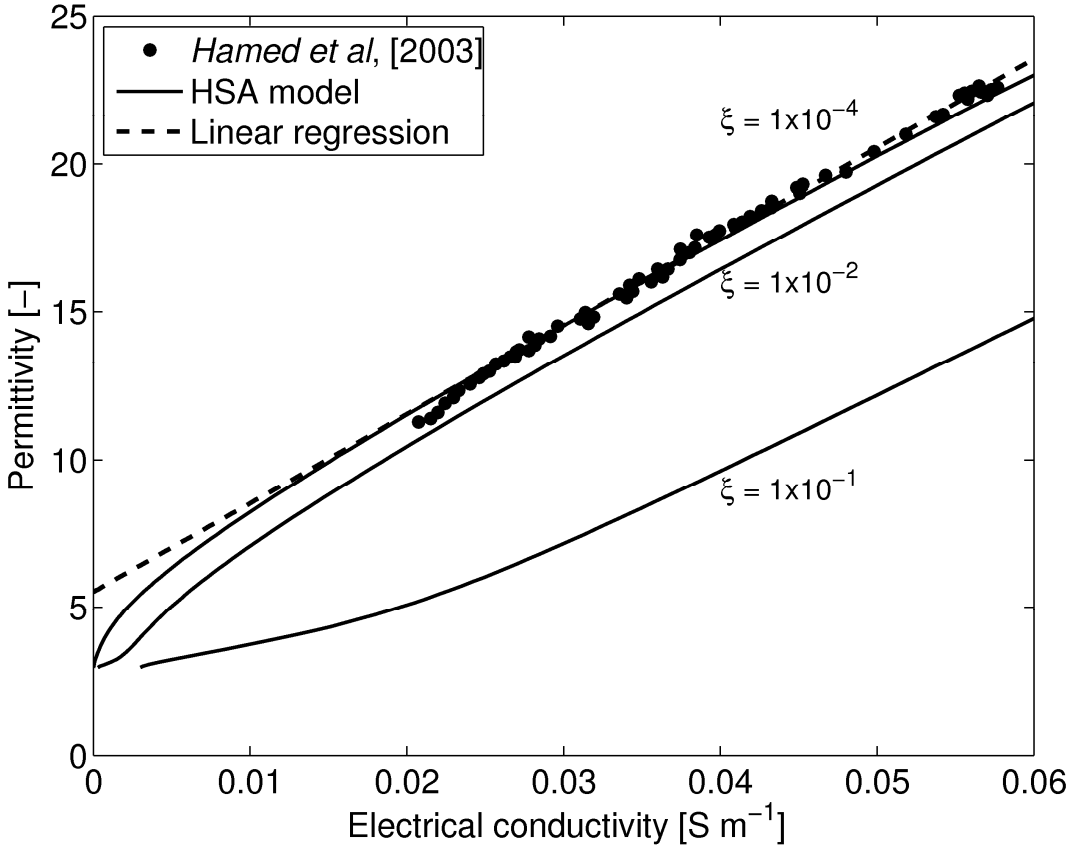

886

887 **Figure 9.** Permittivity versus electrical conductivity relationship for an organic top soil. Data from
888 *Hamed et al.* [2003]. The measured electrical conductivity of the pore water was 2.9×10^{-2} S m^{-1}.
889 The value estimated from Eq. 19 using data in the range with linear behavior ( ) was very
890 similar, 2.63×10^{-2} S m^{-1}. This dataset was measured varying the moisture content in the range
891 .

892

893

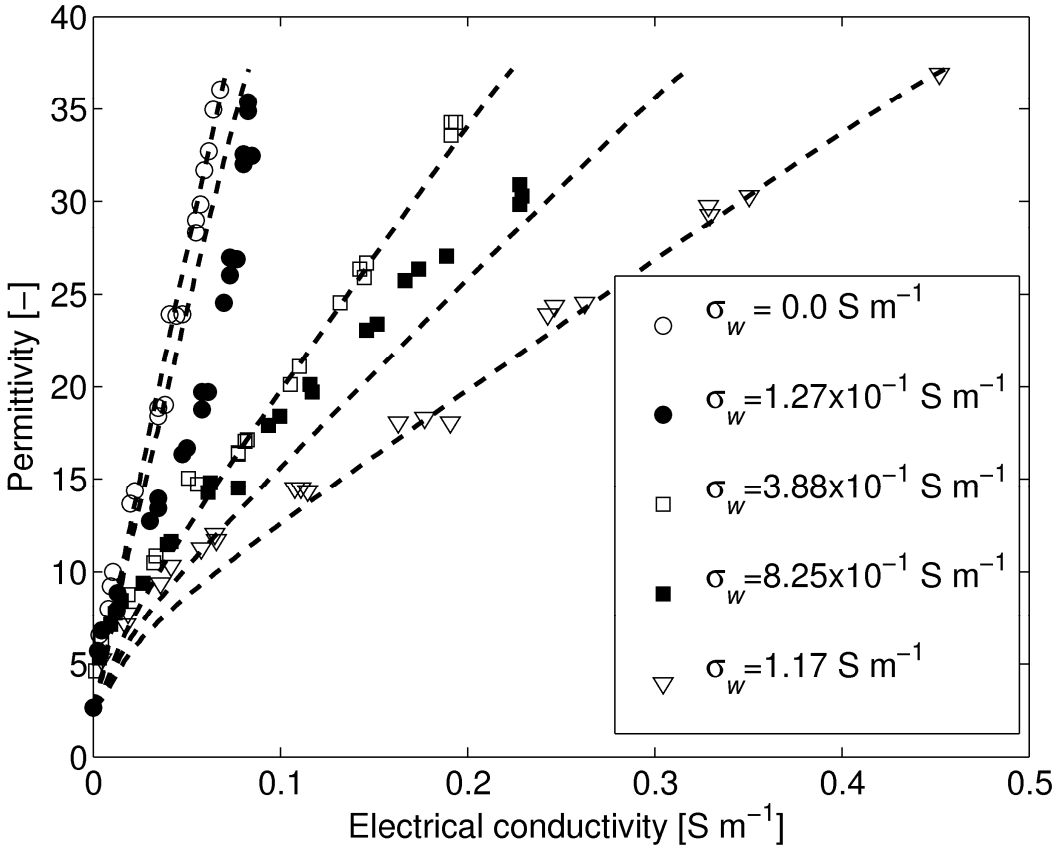

Figure 10. Electrical conductivity vs. permittivity for a clayey soil (experimental data from *Malicki and Walczak*, [1999]). The 5 datasets are relevant to the same soil sample at increasing conductivity of the pore water. The dashed line is the HSA constitutive model presented in this work. The same parameters (texture, solid phase permittivity and surface conductivity) were used to fit all datasets. Pore-water conductivity was estimated using the linear approximation approach, because it was not possible to match some datasets using the measured values. The model parameters are reported in Table 1 and predicted vs. measured water conductivities are reported and compared in Table 3.